



## Rapid and robust modification of PVDF ultrafiltration membranes with enhanced permselectivity, antifouling and antibacterial performance

Kai Cheng<sup>1</sup>, Na Zhang<sup>1</sup>, Na Yang<sup>\*</sup>, Shuai Hou, Jiahui Ma, Luhong Zhang, Yongli Sun, Bin Jiang

School of Chemical Engineering and Technology, Tianjin University, Tianjin 300072, PR China

### ARTICLE INFO

#### Keywords:

Ultrafiltration  
Antifouling  
Antibacterial  
Dopamine  
Micromolecular zwitterion

### ABSTRACT

Zwitterionic materials are well known to possess extraordinary water affinity. However, micromolecular zwitterions have rarely been exploited for membrane hydrophilic modification. Herein, novel antifouling and antibacterial polyvinylidene fluoride (PVDF) ultrafiltration membranes with enhanced permselectivity were facilely fabricated through one-step co-deposition of dopamine and a newly synthesized micromolecular zwitterion (DMAPAPS). With the assistance of  $\text{CuSO}_4/\text{H}_2\text{O}_2$ -triggered oxidation, a uniform and hydrophilic coating (water contact angle =  $33^\circ$ ) was constructed on membrane surface in only 40 min. The impacts of the DMAPAPS concentration and coating time on membrane performance were investigated. Results showed that our strategy endowed the optimized membrane with high pure water flux of  $364 \text{ L/m}^2 \cdot \text{h}$  and BSA rejection of 98.6%. The flux recovery ratios of membrane were as high as 96.3% for bovine serum albumin, 98.1% for humic acid and 95.1% for sodium alginate after 3-cycle filtration, respectively. Moreover, the membrane displayed superior antibacterial activity towards *E. coli* and *S. aureus* as well as excellent chemical and mechanical stability. This work provides a versatile platform for the robust, time-saving and cost-effective fabrication of antifouling and antibacterial membranes.

### 1. Introduction

Ultrafiltration (UF) process, which plays a vital role in membrane technology, has been broadly applied for water purification [1,2]. As one of the most commonly used membrane materials, polyvinylidene fluoride (PVDF) has drawn much attention from researchers due to its high mechanical strength, excellent thermal stability and chemical resistance [3–6]. However, the inherent high hydrophobicity of PVDF membranes makes them prone to be contaminated by organic foulants (such as proteins) and biofoulants (such as bacteria) during filtration [7–9], which leads to dramatic flux decline and undesired shortening of membrane lifetime. Therefore, enhancing the antifouling property of PVDF membrane is essential for its long-term application and large-scale industrialization. Over the past decades, it has been proved that hydrophilic modification is an effective way to alleviate membrane fouling propensity [10–12]. Thus, various typical modification methods, such as surface coating [13,14], surface grafting [15,16], physical blending [17–19], surface segregation [6,20,21] and surface bio-adhesion

[22,23] have been explored to fabricate hydrophilic membranes. For example, in Fu et al.'s work [24], antifouling PVDF UF membrane was prepared by grafting a hydrophilic poly(N-acryloyl glycinamide) (PNAGA) hydrogel via UV-initiated radical graft polymerization and its flux recovery ratio (FRR) was as high as 99% after cyclic filtration of BSA solution. Yang et al. [25] fabricated a hydrophilic PVDF UF membrane by blending PVDF with a fluoro-contained polymer (SPTFS), which exhibited improved antifouling property with FRR of 56.9% and increased permeability with pure water flux of above  $300 \text{ L/m}^2 \cdot \text{h}$ .

Among the aforementioned membrane modification techniques, mussel-inspired surface bio-adhesion has moved into the spotlight attributed to its simplicity, versatility, robustness and low toxicity since this concept was first proposed in 2007 [26–28]. As one of the most renowned mussel-inspired adhesives, dopamine (DA), which is able to adhere tightly to almost all kinds of solid surfaces under alkaline conditions [29,30], has been intensively employed for surface hydrophilic modification. In addition, the oxidized DA can also be bonded with some functional molecules (SH- or  $\text{NH}_2$ -based materials mainly) following the

\* Corresponding author.

E-mail address: [yangnayna@tju.edu.cn](mailto:yangnayna@tju.edu.cn) (N. Yang).

<sup>1</sup> Kai Cheng and Na Zhang are co-first authors.

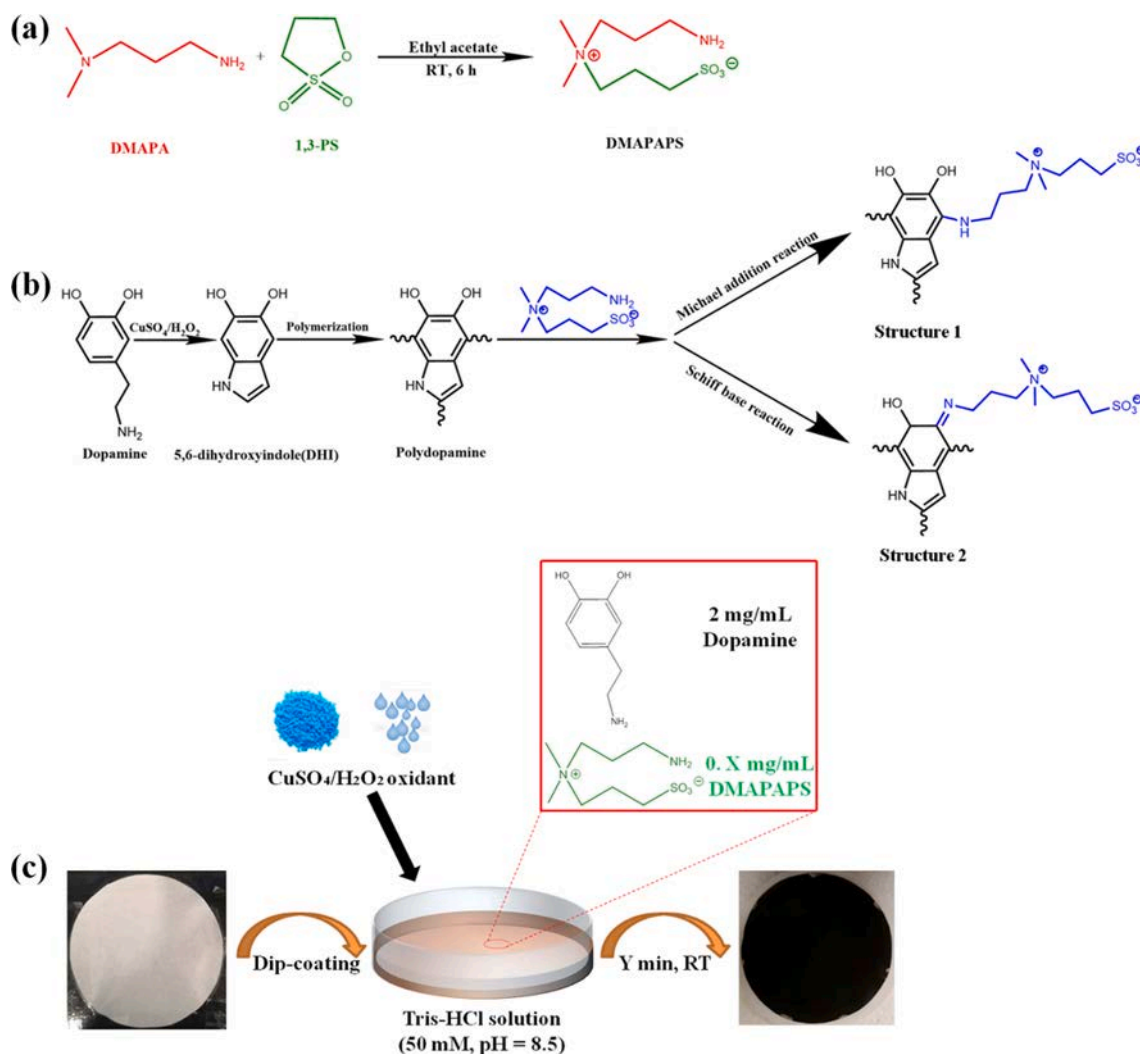


**Fig. 1.** (a) Synthesis of zwitterionic DMAPAPS; (b) proposed mechanism of dopamine polymerization triggered by  $\text{CuSO}_4/\text{H}_2\text{O}_2$  and its subsequent reaction with DMAPAPS [49]; (c) schematic illustration of membrane modification.

Michael addition or Schiff base reaction pathways [29,31], which has undoubtedly opened an avenue to further enhance the surface hydrophilicity of membranes. For instance, Freeman et al. [32] modified a UF membrane through DA deposition followed by grafting of mPEG-NH<sub>2</sub>, after which the as-prepared membrane showed enhanced hydrophilicity (WCA = ~ 35°) and oil/water fouling resistance. Lin et al. [33] grafted amine-terminated polysiloxane onto the polydopamine-coated ultrafiltration membranes, which endowed the surfaces with higher antifouling capacity. In recent years, a great deal of reports have revealed that zwitterionic materials, which possess equivalent cationic and anionic sites, normally show stronger hydration ability and superior antifouling performance than the neutrally charged hydrophilic polymers [34–37]. In the study of Xu's work [38], highly hydrophilic (WCA < 20°) and antifouling (FRR > 80%) membrane surface was facilely constructed through co-deposition of zwitterionic poly(sulfobetaine methacrylate) and dopamine. Sheiko et al. [39] fabricated a substrate-independent hydrophilic coating via copolymerization of zwitterionic SBMA and dopamine methacrylamide monomers, which exhibited distinct antifouling and antifogging performances. In comparison with long-chain zwitterionic polymers, micromolecular zwitterions possess the merits of excellent solubility, good processability and low cost of synthesis [40–42]. Nevertheless, up to now, micromolecular zwitterions have rarely been employed for membrane surface modification.

Although surface bio-adhesion strategy provides a versatile platform

for membrane modification, the deposition of polydopamine (PDA) on substrates is generally a time-consuming process (>24 h) in the ambient air [22]. Therefore, a variety of chemical oxidants, such as  $\text{CuSO}_4$  [43],  $\text{NaIO}_4$  [44],  $(\text{NH}_4)_2\text{S}_2\text{O}_8$  [45],  $\text{KMnO}_4$  [46] and  $\text{CuSO}_4/\text{H}_2\text{O}_2$  [47], have been intensively exploited to accelerate the oxidation and polymerization of DA over the past decade. Among them, the  $\text{CuSO}_4/\text{H}_2\text{O}_2$ -triggered method shows distinct advantages through which PDA displays great deposition rate and the formed coating possesses comparatively high stability in both acidic and alkaline media. On the basis of the above analysis, it is hopeful to develop a robust, time-saving, and economical approach to fabricate antifouling membranes through a proper selection of oxidants and modifiers.

In this work, a micromolecular zwitterion (DMAPAPS) containing amino and quaternary ammonium groups was synthesized through ring-opening reaction. Hydrophobic PVDF UF membrane was facilely modified by the rapid one-step co-deposition of DA and DMAPAPS with the assistance of  $\text{CuSO}_4/\text{H}_2\text{O}_2$  oxidation. Two control experiments, of which the dipping solutions were in the absence of either  $\text{CuSO}_4/\text{H}_2\text{O}_2$  or DMAPAPS, were also set to probe the impact of oxidant and zwitterion on the performance of modified membranes, respectively. The membrane surfaces were characterized by attenuated total reflectance Fourier transform infrared spectroscopy (ATR-FTIR), X-ray photoelectron spectroscopy (XPS), scanning electron microscope (SEM), atomic force microscope (AFM) and water contact angle (WCA) test. The

separation performance, antifouling and antibacterial property as well as stability of membranes were systematically investigated.

## 2. Experimental

### 2.1. Materials

Commercial PVDF ultrafiltration membranes (UF50, MWCO = 50 kDa) were supplied by Shanghai Hengyi membrane Environmental Protection Technology Co., Ltd. (Shanghai, China). Dopamine hydrochloride (DA-HCl, 98%), 3-Dimethylaminopropylamine (DMAPA, 99%), 1, 3-Propanesultone (1, 3-PS, 99%), copper(II) sulfate pentahydrate (CuSO<sub>4</sub>·5H<sub>2</sub>O, AR), hydrogen peroxide solution (30%, AR), ethanol (EtOH, AR), ethyl acetate (AR), humic acid (HA, AR) and sodium alginate (SA, AR) were purchased from Shanghai Aladdin Reagent Company (Shanghai, China). Bovine serum albumin (BSA, 68 kDa) was supplied by Beijing solarbio science & technology Co., Ltd. (Beijing, China). Tris (hydroxymethyl)-aminomethane buffer (Tris-HCl, 1 M, pH = 8.5) and phosphate buffer saline (PBS, 1 M, pH = 7) were obtained from Senbeijia biological technology Co., Ltd. (Nanjing, China). Deionized water was used in all experiments. All the chemicals were used as received without any further purification.

### 2.2. Synthesis of zwitterion (DMAPAPS)

Sulfonated 3-Dimethylaminopropylamine (DMAPAPS) was synthesized by the ring-opening reaction [48] of 1, 3-PS with DMAPA as shown in Fig. 1a. Specifically, DMAPA (5.11 g) and ethyl acetate (60 mL) were put into a 250 mL round bottom flask equipped with a stirrer at ambient temperature. Then, a mixture of 1, 3-PS (6.11 g) and ethyl acetate (20 mL) was added dropwise into the stirred solution for at least 30 min. The reaction was remained for another 6 h under room temperature and the transparent solution gradually turned into milky white suspension. The product was then collected by filtration and washed by ethyl acetate repeatedly for thoroughly removing the unreacted chemicals. Finally, the white solid was dried under vacuum at 50 °C for 24 h for further use. The successful synthesis of DMAPAPS was confirmed by NMR (Bruker, Germany, 400 MHz) and MS results (Agilent 6120, US) shown in Figs. S1 and S2, respectively. <sup>1</sup>H NMR (solvent: D<sub>2</sub>O): δ/ppm = 3.10 (m, 2H, NH<sub>2</sub>CH<sub>2</sub>CH<sub>2</sub>CH<sub>2</sub>), 2.94 (m, 2H, CH<sub>2</sub>CH<sub>2</sub>CH<sub>2</sub>SO<sub>3</sub><sup>-</sup>), 2.85 (s, 6H, N<sup>+</sup>(CH<sub>3</sub>)<sub>2</sub>), 2.56 (t, 2 × 2H, NH<sub>2</sub>CH<sub>2</sub> and CH<sub>2</sub>SO<sub>3</sub><sup>-</sup>), 1.98 (m, 2H, NH<sub>2</sub>CH<sub>2</sub>CH<sub>2</sub>) and 1.87 (m, 2H, CH<sub>2</sub>CH<sub>2</sub>SO<sub>3</sub><sup>-</sup>). MS (mass/charge ratio): 223.1 ([M-H<sup>+</sup>]).

### 2.3. Fabrication of composite PVDF membranes

The pristine PVDF membranes were firstly soaked in ethanol for 30 min to remove the residual chemicals within the pores, and then rinsed with deionized water for 24 h to completely wash away the ethanol. The pretreated bare membranes were denoted as M0. For the one-step co-deposition experiment (Fig. 1c), a certain amount of DMAPAPS and 0.1 g of DA were co-dissolved into a 50 mL Tris-HCl buffer solution (50 mM, pH = 8.5), within which the concentration of CuSO<sub>4</sub>/H<sub>2</sub>O<sub>2</sub> oxidant was determined at 5 mM/19.6 mM [48]. Afterwards, the obtained solution was poured onto the surface of M0 and shaken on a shaker for a designed time. Finally, the membranes were thoroughly rinsed and restored in deionized water before use. The as-modified membranes above were labeled as M-X-Y, where X represented the concentration (0.X mg/mL) of DMAPAPS in dipping solution and Y represented the coating time (Y min), respectively. For comparison, the membranes modified with no CuSO<sub>4</sub>/H<sub>2</sub>O<sub>2</sub> oxidant or DMAPAPS were also fabricated and named as M'-X-Y and M-0-Y, respectively. The modification conditions for all membranes involved in this paper are summarized in Table S1. The photographs of some selected membranes are displayed in Fig. S3. All the experiments were carried out at room temperature with a constant shaking rate of 80 rpm.

### 2.4. Characterization

A UV-vis spectrometer (UV-4802S, Unico, US) was employed to detect the evolution of DA in different solutions. Surface chemical composition of membranes was characterized by attenuated total reflectance Fourier transform infrared spectroscopy (ATR-FTIR, Spectrum 100, Perkin Elmer, US) and X-ray photoelectron spectroscopy (XPS, 250xi, Thermo ESCALAB, US). Surface morphology and roughness of membranes were characterized by scanning electron microscopy (SEM, Hitachi, S4800, Japan) and atomic force microscopy (AFM, Dimension icon, Bruker, Germany), respectively. The porosity (ε, %) and mean pore size (r<sub>m</sub>) of membranes were obtained by the gravimetric method [50] and filtration velocity method [51], respectively. Zeta potential of membrane surfaces at a fixed pH of 7 was determined by an electrokinetic analyzer (Surpass, Anton Paar, Austria). Surface hydrophilicity of membranes was assessed by the water contact angle (WCA) tests conducted on a goniometer (JC 2000, Powereach, China) with a constant drop volume of 2.5 μL.

### 2.5. Separation performance of membranes

The filtration experiments were conducted in a dead-end filtration unit with an effective filtration area of 33.18 cm<sup>2</sup>. Prior to testing, the membranes were compacted with deionized water at 1.5 bar for 30 min to get a steady flux. Afterwards, the pressure was adjusted to 1 bar and the pure water flux (PWF) was obtained by Eq. (1):

$$J = \frac{V}{A\Delta t} \quad (1)$$

where  $J$ ,  $V$ ,  $A$  and  $\Delta t$  correspond to the flux (L/m<sup>2</sup>·h), volume of permeate (L), effective filtration area (m<sup>2</sup>) and permeation time (h), respectively.

The selectivity of membranes was evaluated by filtrating 1 g/L BSA solution at room temperature, of which the BSA concentration was detected by a UV-vis spectrophotometer (UV-4802S, Unico, USA) at the wavelength of 280 nm. The BSA rejection ( $R$ ) was calculated by the following equation:

$$R = \left(1 - \frac{C_p}{C_f}\right) \times 100\% \quad (2)$$

where  $C_p$  and  $C_f$  refer to the concentrations of BSA in the permeate and feed side, respectively.

### 2.6. Antifouling tests

Cyclic filtration experiments were carried out to evaluate the anti-fouling performance of membranes using HA, BSA and SA as the model foulants. To start with, the PWF of membrane was recorded for 30 min at 1 bar. Subsequently, a PBS solution (10 mM, pH = 7) containing 1 g/L of foulant was filtered for 30 min under the same pressure. Then, the fouled membrane was thoroughly cleaned by washing and backwashing with deionized water for 10 min and the PWF was tested again for another 30 min. The above cycle was repeated for three times. The flux recovery rate ( $FRR$ ), reversible fouling ratio ( $R_r$ ) and irreversible fouling ratio ( $R_{ir}$ ) were applied to assess the fouling-resistance of membranes which were defined by Eqs. (3)–(5):

$$FRR = \frac{J_{w2}}{J_{w1}} \times 100\% \quad (3)$$

$$R_r = \frac{J_{w2} - J_p}{J_{w1}} \times 100\% \quad (4)$$

$$R_{ir} = \frac{J_{w1} - J_{w2}}{J_{w1}} \times 100\% \quad (5)$$

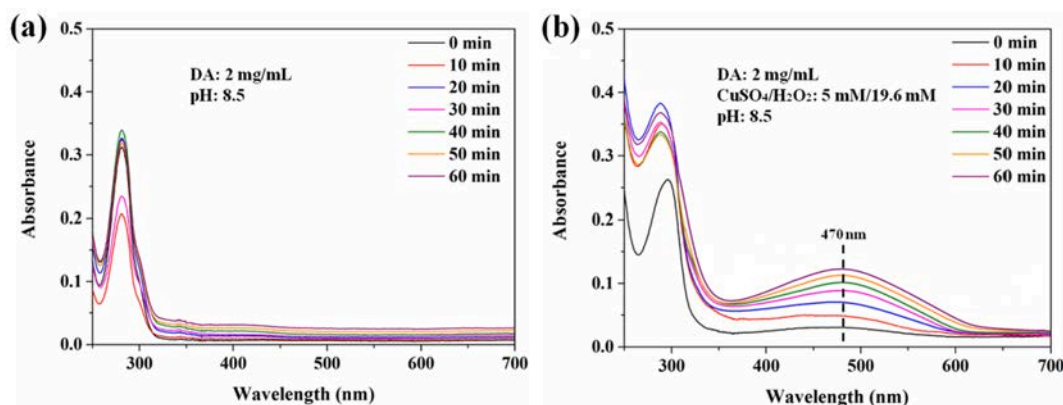


Fig. 2. UV-vis spectra of DA solutions under (a) air oxidation and (b)  $\text{CuSO}_4/\text{H}_2\text{O}_2$  oxidation.

where  $J_{w1}$  is the initial pure water flux,  $J_{w2}$  is the recovered pure water flux ( $\text{L}/\text{m}^2\cdot\text{h}$ ) of the third cycle and  $J_p$  is the filtration flux of foulant solution of the third cycle.

### 2.7. Antibacterial tests

Gram-negative (*E. coli*) and Gram-positive bacteria (*S. aureus*) were used as model bio-foulants for the evaluation of membrane antibacterial property. To start with, a membrane sample ( $3 \times 3$  cm) was placed in a petri dish and sterilized with UV light for 30 min. Then, 300  $\mu\text{L}$  of bacteria solution with a cell concentration of  $2 \times 10^6$  CFU/mL was added on the membrane surface and incubated at  $37^\circ\text{C}$  for 24 h. Following the incubation, the bacteria were removed from the membrane surface and transferred into a 50 mL PBS solution ( $\text{pH} = 7.4$ ). Afterwards, the bacteria solution was spread on an agar plate and incubated for another 24 h at  $37^\circ\text{C}$ . Finally, the bacteria colonies were counted and the antibacterial rate was determined by Eq. (6) [52]:

$$\text{Antibacterial rate}(\%) = \left( \frac{N_p - N_m}{N_p} \right) \times 100 \quad (6)$$

where  $N_p$  and  $N_m$  represent the number of visible bacterial colonies on the agar plate after contacting with the pristine and modified membranes, respectively.

### 2.8. Stability tests

The chemical stability of modified membrane was evaluated under different PH environments. In short, a membrane sample was first immersed into the neutral ( $\text{pH} = 7$ ), strong acidic ( $\text{pH} = 2$ ) and strong basic ( $\text{pH} = 12$ ) solutions for 12 h, respectively, followed by recording its water contact angle variations.

The mechanical stability of membrane was also investigated: for each cycle, the membrane was initially subjected to 1 min of sonication (240 W, 40 KHz), and then its PWF and BSA rejection were measured, respectively. The above process was repeated for 10 times to see the changes.

## 3. Results and discussion

### 3.1. $\text{CuSO}_4/\text{H}_2\text{O}_2$ -induced polymerization of DA

It is generally recognized that the formation mechanism of PDA coatings on substrates typically involves the oxidative polymerization of DA [22,43,45]. Herein, the reactivity of DA under different conditions was detected by UV-vis spectra at room temperature. As shown in Fig. 2, compared with the pure DA aqueous solutions (2 mg/L,  $\text{pH} = 8.5$ , diluted by 50 times when sampling, the same below), solutions

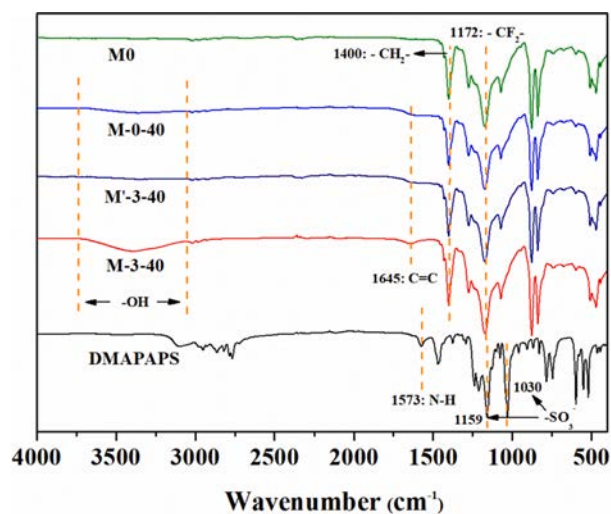


Fig. 3. ATR-FTIR spectra of the membranes.

containing 5 mM/19.6 mM of  $\text{CuSO}_4/\text{H}_2\text{O}_2$  presented an extra strong peak at around 470 nm in a short time, which was ascribed to the fast oxidative cyclization and polymerization of DA [44,47]. The above results demonstrate that  $\text{CuSO}_4/\text{H}_2\text{O}_2$  could act as a powerful oxidant to achieve the rapid oxidation and polymerization of DA. The proposed mechanism of DA polymerization triggered by  $\text{CuSO}_4/\text{H}_2\text{O}_2$  is shown in Fig. 1b.

### 3.2. Surface chemical composition of membranes

ATR-FTIR and XPS were applied to analyze the surface chemical composition of membranes. As shown in the ATR-FTIR spectra (Fig. 3), in contrast to the pristine membrane (M0), the modified membranes all exhibited two extra peaks at 1645 and 3050–3750  $\text{cm}^{-1}$ , ascribed to the aromatic stretching vibration of  $\text{C} = \text{C}$  and  $-\text{OH}$ , respectively [53,54], indicating that PDA was successfully deposited on membrane surfaces. However, the characteristic peaks of DMAPAPS did not appear in M-3-40. This might be because that the amount of DMAPAPS immobilized on membrane surfaces was limited and the peaks were likely to be covered by the intrinsic strong peaks of PVDF [42].

As seen in the XPS spectra (Fig. 4a), with comparison to the pristine membrane (M0), all the modified membranes showed two new peaks of N 1s and O 1s, which were mainly stemmed from the amino and catechol groups of PDA coating. Additionally, M-3-40 and M'-3-40 appeared an extra peak of S 2p, confirming that DMAPAPS was immobilized on membrane surfaces. As shown in Table 1, the N/F ratio of both M-0-40

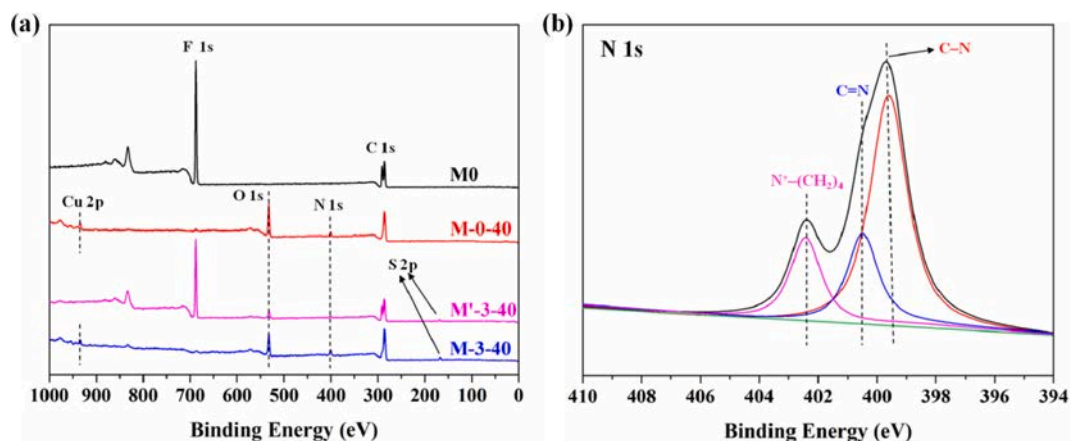


Fig. 4. (a) XPS wide-scan spectra of different membranes and (b) the high-resolution N 1s spectrum of M-3-40.

**Table 1**  
Elemental analysis of the membrane surfaces.

Membrane	Composition (%)						Element ratio N/F
	C	N	O	F	S	Cu	
M0	52.1			47.9			
M'-3-40	57.8	3.2	6.8	31.8	0.4		0.1
M-0-40	62.1	6.9	26.6	2.6		1.8	2.7
M-3-40	60.7	7.5	26.0	2.8	1.5	1.5	2.7

and M-3-40 (2.7) was much higher than that of M'-3-40 (0.1), demonstrating that the deposition of PDA could be dramatically accelerated by the  $\text{CuSO}_4/\text{H}_2\text{O}_2$  oxidant. The high-resolution N 1s spectra of M-3-40 is shown in Fig. 4b. As seen, the peaks at 399.7 eV, 400.5 eV and 402.4 eV were assigned to C-N, C = N and  $\text{N}^+(\text{CH}_2)_4$ , respectively [55], suggesting that DMAPAPS was chemically bonded with PDA following Michael addition and Schiff base reaction pathways (illustrated in Fig. 1a).

### 3.3. Morphology of membranes

SEM and AFM characterizations were employed to analyze the surface morphology of membranes. As exhibited in Fig. 5a and 5b, the surface of M'-3-40 showed no obvious change compared to that of the pristine membrane (M0), indicating that very limited amount of PDA-DMAPAPS was deposited on membrane surface under air oxidation. By comparison, both M-0-40 and M-3-40 exhibited noticeable pore size shrinkage as observed in Fig. 5c and 5d, demonstrating that adequate PDA layers were formed in a short time with the assistance of  $\text{CuSO}_4/\text{H}_2\text{O}_2$  oxidation. This was in well accordance with the mean pore size

results (Fig. S4), of which the average pore diameter of M-0-40 (25.8 nm) and M-3-40 (26.2 nm) was much smaller than that of M0 (52.3 nm) and M'-3-40 (50.7 nm). Besides, all of the modified membranes showed a similar porosity to the pristine membrane (Fig. S4), suggesting that the internal pore structure of membranes was hardly affected by the PDA or PDA-DMAPAPS coatings.

From the AFM images, it can be seen that, in contrast to M0 ( $R_a = 21.6$  nm), all the PDA-coated membranes exhibited an increased surface roughness. There into, the roughness of M-0-40 ( $R_a = 28.8$  nm) and M-3-40 ( $R_a = 30.3$  nm) was relatively lower than that of M'-3-40 ( $R_a = 35.1$

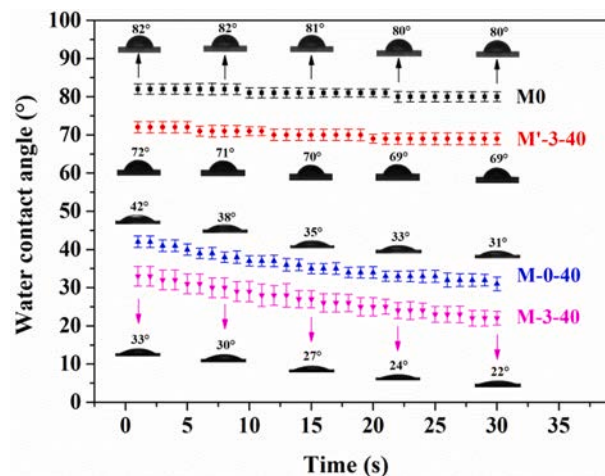


Fig. 6. Water contact angles of the prepared membranes.

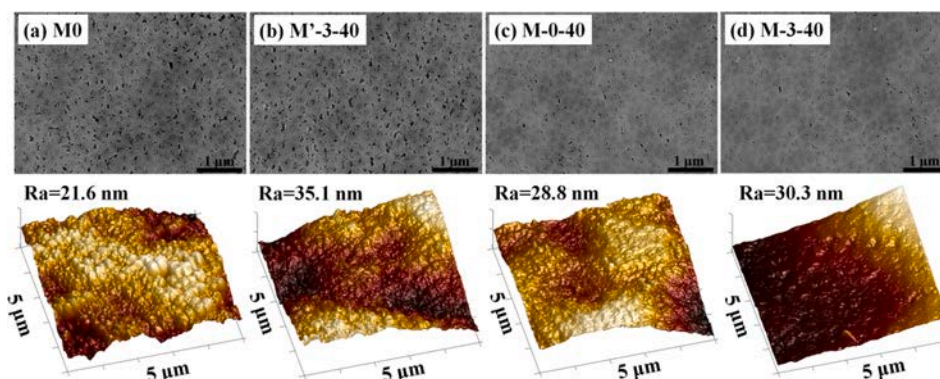
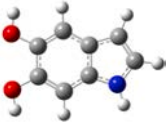
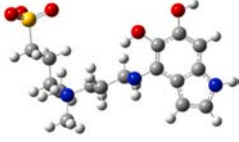


Fig. 5. Surface SEM images of (a) M0, (b) M'-3-40, (c) M-0-40 and (d) M-3-40, and the below is the corresponding AFM image.

**Table 2**  
Properties of different molecules in the coatings.

Molecule (segment)	Optimized structure <sup>a</sup>	Gibbs free energy of dissolution <sup>a</sup> (kJ/mol)
PDA		-17.41
PDA-DMAPAPS (structure 1)		-61.67
PDA-DMAPAPS (structure 2)		-57.72

<sup>a</sup> Results were given by the Gaussian 09 program at the M062X/6-311 + g(d, p) level.

nm), suggesting that the employment of  $\text{CuSO}_4/\text{H}_2\text{O}_2$  could facilitate the uniform deposition of PDA on substrates [47]. Moreover, the EDS mapping images of M-3-40 shown in Fig. S5 illustrated that the N, O, S and Cu elements were homogeneously distributed on membrane surface, which further confirmed that a PDA-DMAPAPS coating was uniformly constructed after modification.

### 3.4. Surface hydrophilicity of membranes

The surface hydrophilicity of membranes modified through different approaches was characterized by water contact angle (WCA) tests. As shown in Fig. 6, WCA of the pristine membrane (M0) was stabilized at around  $80^\circ$  within 30 s due to its inherent low hydrophilicity. After co-deposition of DA and DMAPAPS under air oxidation, M'-3-40 showed slightly improved hydrophilicity with an initial WCA of  $72^\circ$ , which was ascribed to the limited amount of hydrophilic PDA-DMAPAPS coating on

membrane surface (see Sections 3.2 and 3.3). Upon the individual deposition of DA through  $\text{CuSO}_4/\text{H}_2\text{O}_2$  oxidation, M-0-40 possessed a more hydrophilic surface and the WCA gradually declined from  $42^\circ$  to  $31^\circ$  in 30 s. Moreover, M-3-40 exhibited the highest hydrophilicity with WCA decreasing from  $33^\circ$  to  $22^\circ$  within 30 s, indicating that the introduction of DMAPAPS could further enhance the hydrophilicity of PDA coating.

The superior water affinity of PDA-DMAPAPS was verified theoretically by Gaussian simulation. First, for simplification, micromolecular segments were extracted from PDA and PDA-DMAPAPS polymers. Then, their structures were optimized and Gibbs free energies of dissolution were calculated by the Gaussian 09 program [56] at the M062X/6-311 + g(d, p) level [57]. As listed in Table 2, the PDA-DMAPAPS molecules (structure 1 and structure 2) showed much lower Gibbs free energy of dissolution than PDA, suggesting that the combination of PDA and DMAPAPS did help to significantly increase the hydrophilicity of coating.

### 3.5. Separation performance of membranes

Herein, separation performance of the developed membranes was evaluated by measuring their PWF and BSA rejection. As shown in Fig. 7a, the PWF and BSA rejection ratio of pristine membrane were  $172 \text{ L/m}^2 \cdot \text{h}$  and 92.1%, respectively. Upon modification, both the permeability and selectivity of membranes were apparently enhanced. Additionally, it should be noted that the concentration of DMAPAPS within the dipping solution exerted a significant impact on membrane performance. As seen, at a fixed coating time of 30 min, both the PWF and BSA rejection ratio of membranes increased first and then declined with the increasing DMAPAPS concentration, and the membrane prepared with 0.3 mg/mL DMAPAPS showed the highest PWF ( $\text{M}'\text{-3-30}$ ,  $316 \text{ L/m}^2 \cdot \text{h}$ ) and BSA rejection (98.1%). This might be attributed to the trade-off effect between the hydrophilicity and deposition amount of PDA-DMAPAPS on membrane surfaces: on the one hand, the combination of DMAPAPS and PDA could apparently improve the hydrophilicity of coating; on the other hand, the excessive immobilization of DMAPAPS to PDA might cause significant steric repulsion between PDA-DMAPAPS molecules and result in poor deposition, which could be reflected by the surface color depths of the selected membranes prepared with different DMAPAPS concentrations (Fig. S6).

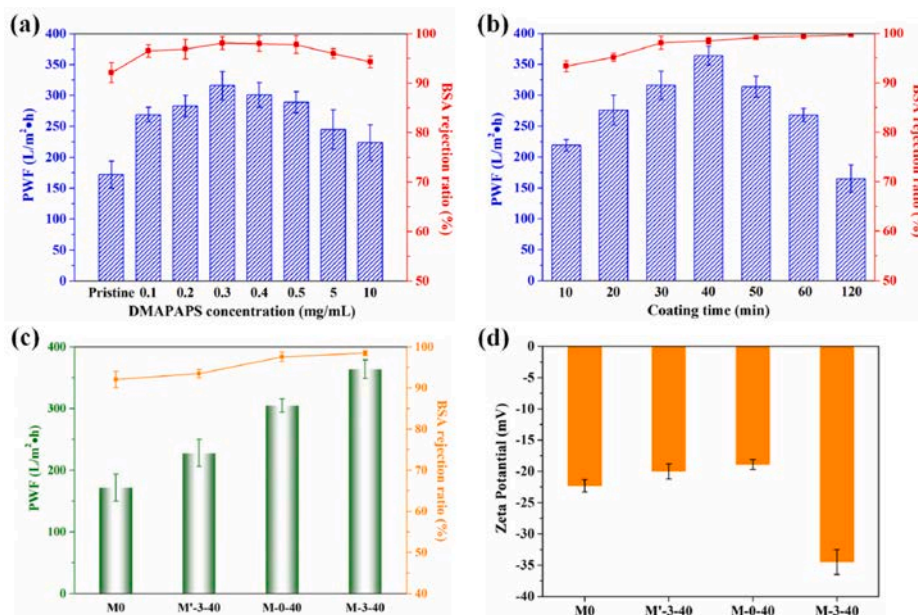


**Fig. 7.** Separation performances of the membranes prepared with (a) different DMAPAPS concentration in dipping solutions (coating time: 30 min) and (b) different coating time (DMAPAPS concentration: 0.3 mg/mL); (c) separation performances and (d) surface zeta potentials of the membranes prepared by different approaches.

**Table 3**

Summarization of separation performance of mussel-inspired ultrafiltration membranes from literatures and this work.

Modification condition	Pure water permeation (L/m <sup>2</sup> ·h·bar)	BSA rejection	Literature
PDA/mPEG-NH <sub>2</sub>	< 100	98.1%	[58]
PDA/TiO <sub>2</sub>	227.9	97%	[59]
GA/APTES	278.2	96.6%	[60]
PDA/PEG	187.4	94.5%	[61]
PDA/TA	490	93%	[62]
PDA/PEI/BSA	71.2	86.8%	[63]
PDA/DMAPAPS	364	98.6%	This work

The coating time was further optimized. As shown in Fig. 7b, when the DMAPAPS concentration in dipping solutions was fixed at 0.3 mg/mL, the PWF of membranes increased first and then decreased with longer coating time. In this case, the increasing hydrophilicity and hydraulic resistance of membrane caused by pore shrinkage might be the main trade-off factors to influence the membrane permeability. Moreover, the BSA rejection ratio of membranes was constantly enhanced as the membrane pores were getting smaller with coating time (Fig. S7). Therefore, M-3-40 (DMAPAPS concentration: 0.3 mg/mL; coating time:

40 min), which showed the highest permeability (364 L/m<sup>2</sup>·h for PWF) and satisfactory selectivity (98.6% for BSA rejection), was screened as the optimized membrane for further investigation.

For comparison, the separation performance of membranes prepared by different approaches was displayed in Fig. 7c. It can be seen that both the PWF and BSA rejection rate followed an order of M-3-40 (364 L/m<sup>2</sup>·h, 98.6%) > M-0-40 (305 L/m<sup>2</sup>·h, 97.6%) > M'-3-40 (228 L/m<sup>2</sup>·h, 93.5%) > M0 (172 L/m<sup>2</sup>·h, 92.1%), which were intensively associated with the surface hydrophilicity (Fig. 6) and MWCO (Fig. S8) of membranes. Besides, the zeta potential results (Fig. 7d) demonstrated that M-3-40 possessed the most negatively charged surface of all, which further strengthened its selectivity since BSA carried a net negative charge in neutral pH solution [24].

Table 3 summarized the separation performance of various mussel-inspired ultrafiltration membranes from relative literatures. As seen, our developed membrane displayed decent pure water permeation (364 L/m<sup>2</sup>·h·bar) and BSA rejection (98.6%), which showed great competitiveness in practical use.

### 3.6. Antifouling performance of membranes

Fig. 8a and 8b exhibited the dynamic flux variations of M0 and M-3-

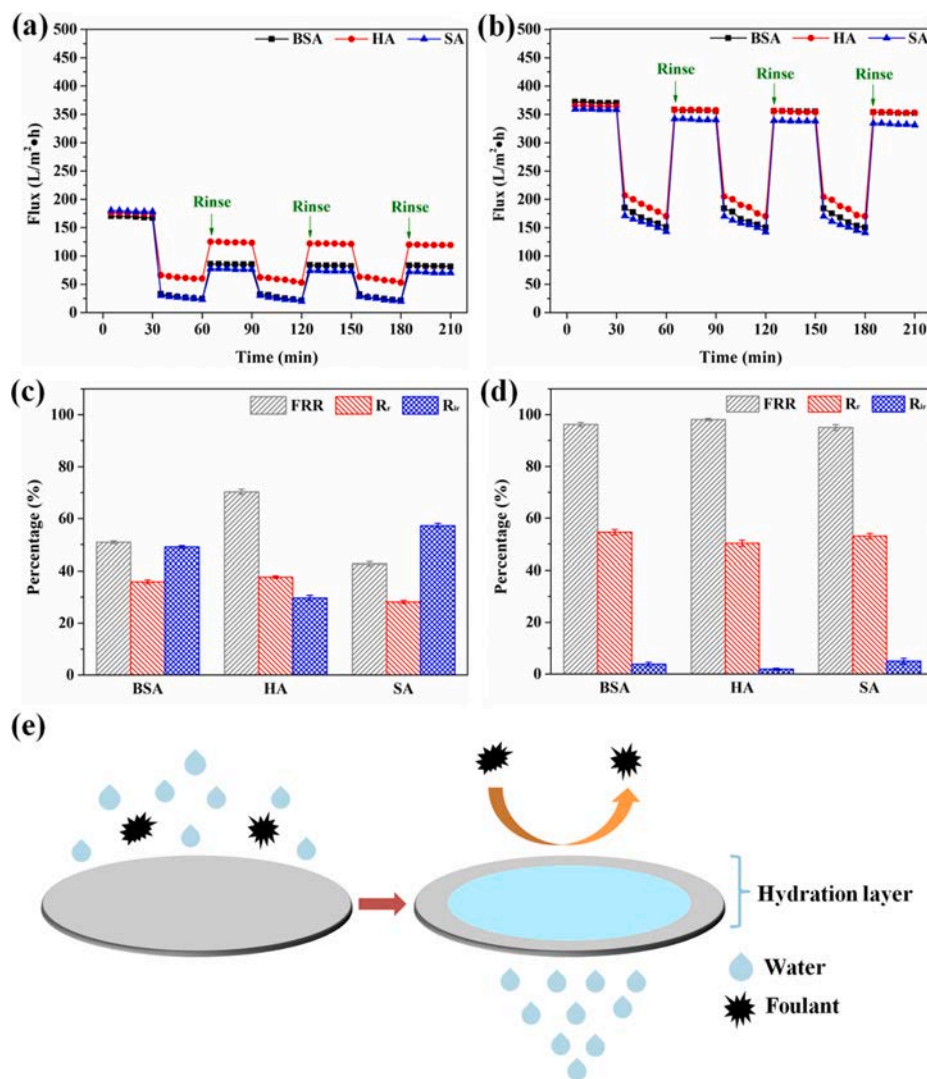


**Fig. 8.** Cyclic filtration tests of the (a) pristine PVDF membrane and (b) M-3-40 using BSA, HA and SA as the model foulants; flux recovery ratio (*FRR*), reversible fouling ratio (*R<sub>r</sub>*) and irreversible fouling ratio (*R<sub>ir</sub>*) of the (c) pristine PVDF membrane and (d) M-3-40 after 3-cycle filtration; (e) schematic illustration for the formation of hydration layer on the surface of M-4-2 when filtrating foulant solutions.

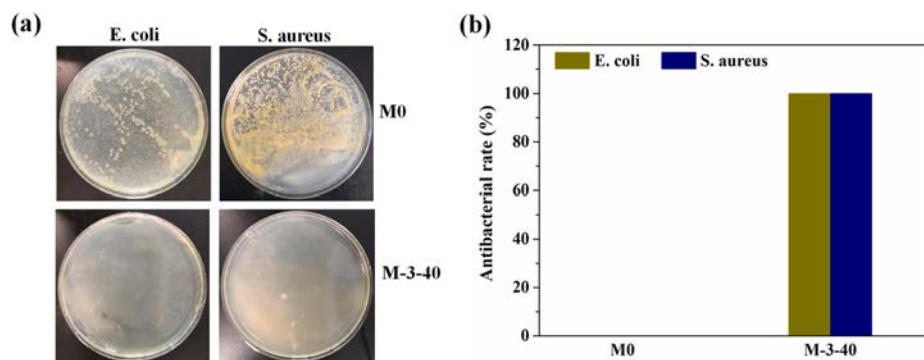


Fig. 9. (a) Photographs of the bacteria colonies after being incubated with M0 and M-3-40 for 24 h, respectively; (b) antibacterial rate of M0 and M-3-40 after incubation.

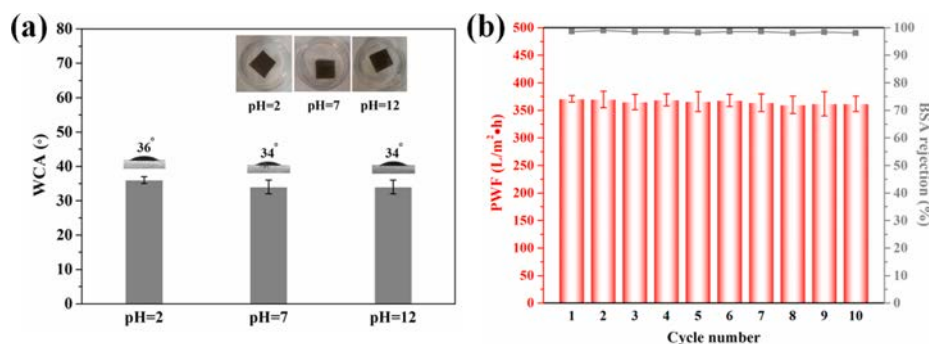


Fig. 10. (a) WCAs of M-3-40 after being subjected to harsh pH solutions; (b) separation performance of M-3-40 during the 10-cycle sonication.

40 during the 3-cycle filtration experiment, respectively. As seen, both of the membranes underwent an obvious flux drop when filtrating foulant solutions, attributed to the formation of filter-cake-layers caused by concentration polarization and foulant deposition [64,65]. The pristine PVDF membrane exhibited poor fouling resistance as the *FRRs* (Fig. 8c) were 50.9%, 70.3% and 42.7% for BSA, HA and SA, respectively, due to the strong interactions between hydrophobic membrane surface and foulants. After modification, as shown in Fig. 8d, M-3-40 showed dramatically improved antifouling performance with high *FRR* (96.3% for BSA, 98.1% for HA and 95.1% for SA) and low  $R_{ir}$  (<5%) values, indicating that the PWF of fouled membrane could be mostly recovered to the initial values through simple water rinsing. This might be ascribed to the compact hydration layer formed on hydrophilic surface which endowed the membrane with excellent fouling-resistance property (illustrated in Fig. 8e).

### 3.7. Antibacterial performance of membranes

Antibacterial performance of membranes was evaluated using Gram-negative (*E. coli*) and Gram-positive bacteria (*S. aureus*) as the model biofoulants. As seen in Fig. 9, the pristine membrane (M0) exhibited no inhibition for the growth of bacteria. Conversely, all of the *E. coli* and *S. aureus* bacteria were killed after being incubated with M-3-40 for 24 h (antibacterial rate = 100%). The excellent antibacterial activity of modified membrane was mainly derived from the copper ions and quaternary ammonium groups existed in the PDA-DMAPAPS coating [66,67].

### 3.8. Stability of membranes

The chemical stability of developed membrane was evaluated under different pH environments. As presented in Fig. 10a, after being subjected to harsh pH solutions (pH = 2, 7 and 12) for 12 h, the

hydrophilicity of M-3-40 showed no obvious variation as its WCAs retained stable at 34°~36°.

For the evaluation of mechanical stability, the separation performance of M-3-40 after each sonication cycle were measured and recorded. As seen in Fig. 10b, the PWF and BSA rejection of membrane were stabilized at around 350 L/m<sup>2</sup>·h and 98% throughout the 10-cycle test, respectively, indicating that the PDA-DMAPAPS coating possessed excellent resistance to physical destruction.

The excellent stability of M-3-40 was probably benefited from the copper ions which acted as crosslink-sites in the coating and strong electrostatic attractions between the PDA-DMAPAPS molecules [42,68].

## 4. Conclusions

In summary, PVDF UF membranes were facily modified through the rapid one-step co-deposition of DA and a newly synthesized micro-molecular zwitterion (DMAPAPS) under the oxidation of CuSO<sub>4</sub>/H<sub>2</sub>O<sub>2</sub>. By this manner, with comparison to the pristine membrane, the modified membrane exhibited much higher hydrophilicity with WCA decreasing from 82° to 33°. As a result, the membrane displayed dramatically improved PWF of 364 L/m<sup>2</sup>·h and BSA rejection of 98.6%, respectively. In addition, the membrane surface possessed excellent fouling resistance to BSA, HA and SA with *FRRs* higher than 95% and  $R_{ir}$  lower than 5% after 3-cycle filtration. The existence of copper ions and quaternary amine groups in the coating endowed the membrane with superior antibacterial property. Moreover, the formed PDA-DMAPAPS coating showed great stability even after being subjected to harsh pH solutions or sonication. This modification strategy holds a promising potential for the fast preparation of high-performance antifouling membranes.

## CRedit authorship contribution statement

**Kai Cheng:** Conceptualization, Methodology, Software, Validation, Investigation, Visualization, Writing - original draft. **Na Zhang:** Methodology, Validation, Formal analysis, Writing - review & editing. **Na Yang:** Validation, Supervision, Data curation, Resources. **Shuai Hou:** Conceptualization, Software, Formal analysis. **Jiahui Ma:** Validation, Formal analysis. **Luhong Zhang:** Supervision, Funding acquisition. **Yongli Sun:** Validation, Writing - review & editing. **Bin Jiang:** Supervision, Project administration.

## Declaration of Competing Interest

The authors declare that they have no known competing financial interests or personal relationships that could have appeared to influence the work reported in this paper.

## Acknowledgements

We are grateful for the financial support from National Key R&D Program of China (No. 2017YFB0602702-02).

## Appendix A. Supplementary material

Supplementary data to this article can be found online at <https://doi.org/10.1016/j.seppur.2021.118316>.

## References

- Q. Li, Q.-Y. Bi, H.-H. Lin, L.-X. Bian, X.-L. Wang, A novel ultrafiltration (UF) membrane with controllable selectivity for protein separation, *J. Membr. Sci.* 427 (2013) 155–167.
- L. Shi, Y. Lei, J. Huang, Y. Shi, K. Yi, H. Zhou, Ultrafiltration of oil-in-water emulsions using ceramic membrane: Roles played by stabilized surfactants, *Colloids Surf. A* 583 (2019), 123948.
- M. Gu, J. Zhang, X. Wang, H. Tao, L. Ge, Formation of poly(vinylidene fluoride) (PVDF) membranes via thermally induced phase separation, *Desalination* 192 (1–3) (2006) 160–167.
- M. Mertens, C. Van Goethem, M. Thijs, G. Koecelberghs, I.F.J. Vankelecom, Crosslinked PVDF-membranes for solvent resistant nanofiltration, *J. Membr. Sci.* 566 (2018) 223–230.
- J. Shen, Q.-i. Zhang, Q. Yin, Z. Cui, W. Li, W. Xing, Fabrication and characterization of amphiphilic PVDF copolymer ultrafiltration membrane with high anti-fouling property, *J. Membr. Sci.* 521 (2017) 95–103.
- B. Saini, D. Vaghani, S. Khuntia, M.K. Sinha, A. Patel, R. Pindoria, A novel stimuli-responsive and fouling resistant PVDF ultrafiltration membrane prepared by using amphiphilic copolymer of poly(vinylidene fluoride) and Poly(2-N-morpholino) ethyl methacrylate, *J. Membr. Sci.* 603 (2020), 118047.
- P.K. Samantaray, G. Madras, S. Bose, PVDF/PBSA membranes with strongly coupled phosphonium derivatives and graphene oxide on the surface towards antibacterial and antifouling activities, *J. Membr. Sci.* 548 (2018) 203–214.
- H. Shi, L. Xue, A. Gao, Y. Fu, Q. Zhou, L. Zhu, Fouling-resistant and adhesion-resistant surface modification of dual layer PVDF hollow fiber membrane by dopamine and quaternary polyethyleneimine, *J. Membr. Sci.* 498 (2016) 39–47.
- G.-D. Kang, Y.-M. Cao, Application and modification of poly(vinylidene fluoride) (PVDF) membranes – A review, *J. Membr. Sci.* 463 (2014) 145–165.
- D. Rana, T. Matsuura, Surface modifications for antifouling membranes, *Chem. Rev.* 110 (4) (2010) 2448–2471.
- R. Zhang, Y. Liu, M. He, Y. Su, X. Zhao, M. Elimelech, Z. Jiang, Antifouling membranes for sustainable water purification: strategies and mechanisms, *Chem. Soc. Rev.* 45 (21) (2016) 5888–5924.
- R.R. Choudhury, J.M. Gohil, S. Mohanty, S.K. Nayak, Antifouling, fouling release and antimicrobial materials for surface modification of reverse osmosis and nanofiltration membranes, *J. Mater. Chem. A* 6 (2) (2018) 313–333.
- Y. Pan, Y. Hang, X. Zhao, G. Liu, W. Jin, Optimizing separation performance and interfacial adhesion of PDMS/PVDF composite membranes for butanol recovery from aqueous solution, *J. Membr. Sci.* 579 (2019) 210–218.
- C. Wei, F. Dai, L. Lin, Z. An, Y. He, X.-i. Chen, L.-i. Chen, Y. Zhao, Simplified and robust adhesive-free superhydrophobic SiO<sub>2</sub>-decorated PVDF membranes for efficient oil/water separation, *J. Membr. Sci.* 555 (2018) 220–228.
- Y. Zhu, J. Wang, F. Zhang, S. Gao, A. Wang, W. Fang, J. Jin, Zwitterionic nanohydrogel grafted PVDF membranes with comprehensive antifouling property and superior cycle stability for oil-in-water emulsion separation, *Adv. Funct. Mater.* 28 (2018) 1804121.
- S. Liang, Y. Kang, A. Tiraferrri, E.P. Giannelis, X. Huang, M. Elimelech, Highly hydrophilic polyvinylidene fluoride (PVDF) ultrafiltration membranes via postfabrication grafting of surface-tailored silica nanoparticles, *ACS Appl. Mater. Interfaces* 5 (14) (2013) 6694–6703.
- S. Liang, K. Xiao, Y. Mo, X. Huang, A novel ZnO nanoparticle blended polyvinylidene fluoride membrane for anti-irreversible fouling, *J. Membr. Sci.* 394–395 (2012) 184–192.
- J. Zhu, S. Zhou, M. Li, A. Xue, Y. Zhao, W. Peng, W. Xing, PVDF mixed matrix ultrafiltration membrane incorporated with deformed rebar-like Fe<sub>3</sub>O<sub>4</sub>-palygorskite nanocomposites to enhance strength and antifouling properties, *J. Membr. Sci.* 612 (2020), 118467.
- A. Xie, J. Cui, J. Yang, Y. Chen, J. Lang, C. Li, Y. Yan, J. Dai, Photo-Fenton self-cleaning PVDF/NH<sub>2</sub>-MIL-88B(Fe) membranes towards highly-efficient oil/water emulsion separation, *J. Membr. Sci.* 595 (2020), 117499.
- A. Venault, Y.-H. Liu, J.-R. Wu, H.-S. Yang, Y. Chang, J.-Y. Lai, P. Aimar, Low-biofouling membranes prepared by liquid-induced phase separation of the PVDF/polystyrene-*b*-poly (ethylene glycol) methacrylate blend, *J. Membr. Sci.* 450 (2014) 340–350.
- H. Sun, X. Yang, Y. Zhang, X. Cheng, Y. Xu, Y. Bai, L. U. Shao, Segregation-induced in situ hydrophilic modification of poly (vinylidene fluoride) ultrafiltration membranes via sticky poly (ethylene glycol) blending, *J. Membr. Sci.* 563 (2018) 22–30.
- Y. Chen, Q. Liu, Oxidant-induced plant phenol surface chemistry for multifunctional coatings: Mechanism and potential applications, *J. Membr. Sci.* 570–571 (2019) 176–183.
- X. Yang, L. Yan, J. Ma, Y. Bai, L. Shao, Bioadhesion-inspired surface engineering constructing robust, hydrophilic membranes for highly-efficient wastewater remediation, *J. Membr. Sci.* 591 (2019), 117353.
- W. Fu, T. Pei, Y. Mao, G. Li, Y. Zhao, L.-i. Chen, Highly hydrophilic poly(vinylidene fluoride) ultrafiltration membranes modified by poly(N-acryloyl glycinamide) hydrogel based on multi-hydrogen bond self-assembly for reducing protein fouling, *J. Membr. Sci.* 572 (2019) 453–463.
- X. Fu, L. Zhu, S. Liang, Y. Jin, S. Yang, Sulfonated poly(α, β, trifluorostyrene)-doped PVDF ultrafiltration membrane with enhanced hydrophilicity and antifouling property, *J. Membr. Sci.* 603 (2020), 118046.
- H. Lee, S.M. Dellatore, W.M. Miller, P.B. Messersmith, Mussel-inspired surface chemistry for multifunctional coatings, *Science* 318 (5849) (2007) 426–430.
- J.H. Ryu, P.B. Messersmith, H. Lee, Polydopamine surface chemistry: a decade of discovery, *ACS Appl. Mater. Interfaces* 10 (9) (2018) 7523–7540.
- X. Zhao, R. Zhang, Y. Liu, M. He, Y. Su, C. Gao, Z. Jiang, Antifouling membrane surface construction: Chemistry plays a critical role, *J. Membr. Sci.* 551 (2018) 145–171.
- W. Cheng, X. Zeng, H. Chen, Z. Li, W. Zeng, L. Mei, Y. Zhao, Versatile polydopamine platforms: synthesis and promising applications for surface modification and advanced nanomedicine, *ACS Nano* 13 (2019) 8537–8565.
- S. Kasemset, A. Lee, D.J. Miller, B.D. Freeman, M.M. Sharma, Effect of polydopamine deposition conditions on fouling resistance, physical properties, and permeation properties of reverse osmosis membranes in oil/water separation, *J. Membr. Sci.* 425–426 (2013) 208–216.
- H. Lee, J. Rho, P.B. Messersmith, Facile conjugation of biomolecules onto surfaces via mussel adhesive protein inspired coatings, *Adv. Mater.* 21 (4) (2009) 431–434.
- B.D. McCloskey, H.B. Park, H. Ju, B.W. Rowe, D.J. Miller, B.D. Freeman, A bioinspired fouling-resistant surface modification for water purification membranes, *J. Membr. Sci.* 413–414 (2012) 82–90.
- T. Tran, X. Chen, S. Doshi, C.M. Stafford, H. Lin, Grafting polysiloxane onto ultrafiltration membranes to optimize surface energy and mitigate fouling, *Soft Matter* 16 (21) (2020) 5044–5053.
- M. He, K. Gao, L. Zhou, Z. Jiao, M. Wu, J. Cao, X. You, Z. Cai, Y. Su, Z. Jiang, Zwitterionic materials for antifouling membrane surface construction, *Acta Biomater.* 40 (2016) 142–152.
- S. Jiang, Z. Cao, Ultralow-fouling, functionalizable, and hydrolyzable zwitterionic materials and their derivatives for biological applications, *Adv. Mater.* 22 (9) (2010) 920–932.
- S. Chen, J. Zheng, L. Li, S. Jiang, Strong resistance of phosphorylcholine self-assembled monolayers to protein adsorption: insights into nonfouling properties of zwitterionic materials, *J. Am. Chem. Soc.* 127 (2005) 14473–14478.
- B. Li, P. Jain, J. Ma, J.K. Smith, Z. Yuan, H.-C. Hung, Y. He, X. Lin, K. Wu, J. Pfandtner, S. Jiang, Trimethylamine N-oxide-derived zwitterionic polymers: A new class of ultralow fouling bioinspired materials, *Sci. Adv.* 5 (6) (2019) eaaw9562, <https://doi.org/10.1126/sciadv.aaw9562>.
- R. Zhou, P.-F. Ren, H.-C. Yang, Z.-K. Xu, Fabrication of antifouling membrane surface by poly(sulfobetaine methacrylate)/polydopamine co-deposition, *J. Membr. Sci.* 466 (2014) 18–25.
- M. Vatankehah-Varnosfaderani, X. Hu, Q. Li, H. Adelnia, M. Ina, S.S. Sheiko, Universal coatings based on zwitterionic-dopamine copolymer microgels, *ACS Appl. Mater. Interfaces* 10 (24) (2018) 20869–20875.
- Q.-F. An, W.-D. Sun, Q. Zhao, Y.-L. Ji, C.-J. Gao, Study on a novel nanofiltration membrane prepared by interfacial polymerization with zwitterionic amine monomers, *J. Membr. Sci.* 431 (2013) 171–179.
- Y.-F. Mi, Q. Zhao, Y.-L. Ji, Q.-F. An, C.-J. Gao, A novel route for surface zwitterionic functionalization of polyamide nanofiltration membranes with improved performance, *J. Membr. Sci.* 490 (2015) 311–320.
- Y. Sun, Y. Zong, N. Yang, N. Zhang, B. Jiang, L. Zhang, X. Xiao, Surface hydrophilic modification of PVDF membranes based on tannin and zwitterionic substance towards effective oil-in-water emulsion separation, *Sep. Purif. Technol.* 234 (2020), 116015.

- [43] F. Bernsmann, V. Ball, Frédéric Addiego, A. Ponche, M. Michel, J.J.d.A. Gracio, Valérie Toniazzo, D. Ruch, Dopamine–melanin film deposition depends on the used oxidant and buffer solution, *Langmuir* 27 (6) (2011) 2819–2825.
- [44] F. Ponzio, J. Barthès, J. Bour, M. Michel, P. Bertani, J. Hemmerlé, M.D. Ischia, V. Ball, Oxidant control of polydopamine surface chemistry in acids: a mechanism-based entry to superhydrophilic-superoleophobic coatings, *Chem. Mater.* 28 (2016) 4697–4705.
- [45] Q. Wei, F. Zhang, J. Li, B. Li, C. Zhao, Oxidant-induced dopamine polymerization for multifunctional coatings, *Polym. Chem.* 1 (9) (2010) 1430, <https://doi.org/10.1039/c0py00215a>.
- [46] Z.M. Tahroudi, A. Razmjou, M. Bagherian, M. Asadnia, Polydopamine surface modification with UV-shielding effect using  $\text{KMnO}_4$  as an efficient oxidizing agent, *Colloids Surf., A* 559 (2018) 68–73.
- [47] C. Zhang, Y. Ou, W. Lei, L. Wan, J. Ji, Z. Xu,  $\text{CuSO}_4/\text{H}_2\text{O}_2$ -induced rapid deposition of polydopamine coatings with high uniformity and enhanced stability, *Angew. Chem., Int. Ed.* 128 (2016) 3106–3109.
- [48] L. Chen, Y. Honma, T. Mizutani, D.-J. Liaw, J.P. Gong, Y. Osada, Effects of polyelectrolyte complexation on the UCST of zwitterionic polymer, *Polymer* 41 (1) (2000) 141–147.
- [49] J. Jiang, L. Zhu, L. Zhu, B. Zhu, Y. Xu, Surface characteristics of a self-polymerized dopamine coating deposited on hydrophobic polymer films, *Langmuir* 27 (23) (2011) 14180–14187.
- [50] B. Chakrabarty, A.K. Ghoshal, M.K. Purkait, Effect of molecular weight of PEG on membrane morphology and transport properties, *J. Membr. Sci.* 309 (1-2) (2008) 209–221.
- [51] Z. Zhang, Q. An, T. Liu, Y. Zhou, J. Qian, C. Gao, Fabrication of polysulfone ultrafiltration membranes of a density gradient cross section with good anti-pressure stability and relatively high water flux, *Desalination* 269 (1-3) (2011) 239–248.
- [52] A. Cihanoğlu, S.A. Altinkaya, A facile route to the preparation of antibacterial polysulfone-sulfonated polyethersulfone ultrafiltration membranes using a cationic surfactant cetyltrimethylammonium bromide, *J. Membr. Sci.* 594 (2020), 117438.
- [53] C. Luo, Q. Liu, Oxidant-induced high-efficient mussel-inspired modification on PVDF membrane with superhydrophilicity and underwater superoleophobicity characteristics for oil/water separation, *ACS Appl. Mater. Interfaces* 9 (9) (2017) 8297–8307.
- [54] J. Jiang, L. Zhu, L. Zhu, H. Zhang, B. Zhu, Y. Xu, Antifouling and antimicrobial polymer membranes based on bioinspired polydopamine and strong hydrogen-bonded poly(N-vinyl pyrrolidone), *ACS Appl. Mater. Interfaces* 5 (24) (2013) 12895–12904.
- [55] S. Zhang, Z. Jiang, X. Wang, C. Yang, J. Shi, Facile method to prepare microcapsules inspired by polyphenol chemistry for efficient enzyme immobilization, *ACS Appl. Mater. Interfaces* 7 (35) (2015) 19570–19578.
- [56] M.J. Frisch, G. Trucks, H.B. Schlegel, G.E. Scuseria, M.A. Robb, J. Cheeseman, G. Scalmani, V. Barone, B. Mennucci, G.A. Petersson, H. Nakatsuji, M. Caricato, X. Li, H.P. Hratchian, A.F. Izmaylov, J. Bloino, G. Zheng, J. Sonnenberg, M. Hada, D. Fox, Gaussian 09 Revision A.1. Gaussian Inc, 2009.
- [57] D. Tzeli, I.D. Petsalakis, G. Theodorakopoulos, D. Ajami, J. Rebek Jr, Theoretical study of free and encapsulated carboxylic acid and amide dimers, *Int. J. Quantum. Chem.* 113 (2013) 734–739.
- [58] C. Cheng, S. Li, W. Zhao, Q. Wei, S. Nie, S. Sun, C. Zhao, The hydrodynamic permeability and surface property of polyethersulfone ultrafiltration membranes with mussel-inspired polydopamine coatings, *J. Membr. Sci.* 417-418 (2012) 228–236.
- [59] L.u. Shao, Z.X. Wang, Y.L. Zhang, Z.X. Jiang, Y.Y. Liu, A facile strategy to enhance PVDF ultrafiltration membrane performance via self-polymerized polydopamine followed by hydrolysis of ammonium fluorotitanate, *J. Membr. Sci.* 461 (2014) 10–21.
- [60] X. Yang, H. Sun, A. Pal, Y. Bai, L.u. Shao, Biomimetic silicification on membrane surface for highly efficient treatments of both oil-in-water emulsion and protein wastewater, *ACS Appl. Mater. Interfaces* 10 (35) (2018) 29982–29991.
- [61] Y. He, L. Xu, X. Feng, Y. Zhao, L. Chen, Dopamine-induced nonionic polymer coatings for significantly enhancing separation and antifouling properties of polymer membranes: Codeposition versus sequential deposition, *J. Membr. Sci.* 539 (2017) 421–431.
- [62] X. Yang, L. Yan, Y. Wu, Y. Liu, L. Shao, Biomimetic hydrophilization engineering on membrane surface for highly-efficient water purification, *J. Membr. Sci.* 589 (2019), 117223.
- [63] J. Wang, S. Gao, X. Kang, J. Tian, F. Cui, W. Shi, One-step synthesis of zwitterionic polyethersulfone ultrafiltration membranes crosslinked by BSA, *Mater. Lett.* 261 (2020), 127007.
- [64] B. Jiang, N.a. Zhang, L. Zhang, Y. Sun, Z. Huang, B. Wang, H. Dou, H. Guan, Enhanced separation performance of PES ultrafiltration membranes by imidazole-based deep eutectic solvents as novel functional additives, *J. Membr. Sci.* 564 (2018) 247–258.
- [65] L. Shi, J. Huang, L. Zhu, Y. Shi, K. Yi, X. Li, Role of concentration polarization in cross flow micellar enhanced ultrafiltration of cadmium with low surfactant concentration, *Chemosphere* 237 (2019), 124859.
- [66] G. Yeroslavsky, M. Richman, L.-o. Dawidowicz, S. Rahimipour, Sonochemically produced polydopamine nanocapsules with selective antimicrobial activity, *Chem. Commun.* 49 (51) (2013) 5721, <https://doi.org/10.1039/c3cc37762h>.
- [67] C.X. Liu, D.R. Zhang, Y. He, X.S. Zhao, R. Bai, Modification of membrane surface for anti-biofouling performance: Effect of anti-adhesion and anti-bacteria approaches, *J. Membr. Sci.* 346 (2010) 121–130.
- [68] S. Kim, T. Gim, S.M. Kang, Stability-enhanced polydopamine coatings on solid substrates by iron(III) coordination, *Prog. Org. Coat.* 77 (8) (2014) 1336–1339.